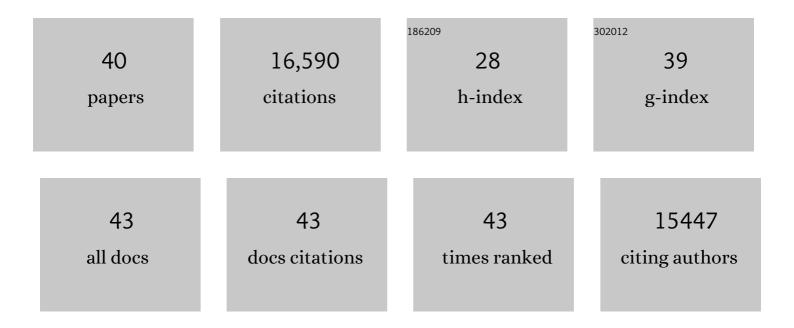
Matthew W Kanan

List of Publications by Year in descending order

Source: https://exaly.com/author-pdf/5235267/publications.pdf Version: 2024-02-01



#	Article	IF	CITATIONS
1	In Situ Formation of an Oxygen-Evolving Catalyst in Neutral Water Containing Phosphate and Co ²⁺ . Science, 2008, 321, 1072-1075.	6.0	3,855
2	CO ₂ Reduction at Low Overpotential on Cu Electrodes Resulting from the Reduction of Thick Cu ₂ O Films. Journal of the American Chemical Society, 2012, 134, 7231-7234.	6.6	1,721
3	Aqueous CO ₂ Reduction at Very Low Overpotential on Oxide-Derived Au Nanoparticles. Journal of the American Chemical Society, 2012, 134, 19969-19972.	6.6	1,462
4	Electroreduction of carbon monoxide to liquid fuel on oxide-derived nanocrystalline copper. Nature, 2014, 508, 504-507.	13.7	1,360
5	Mechanistic Studies of the Oxygen Evolution Reaction by a Cobalt-Phosphate Catalyst at Neutral pH. Journal of the American Chemical Society, 2010, 132, 16501-16509.	6.6	1,074
6	Tin Oxide Dependence of the CO ₂ Reduction Efficiency on Tin Electrodes and Enhanced Activity for Tin/Tin Oxide Thin-Film Catalysts. Journal of the American Chemical Society, 2012, 134, 1986-1989.	6.6	861
7	Cobalt–phosphate oxygen-evolving compound. Chemical Society Reviews, 2009, 38, 109-114.	18.7	683
8	Structure and Valency of a Cobaltâ^'Phosphate Water Oxidation Catalyst Determined by in Situ X-ray Spectroscopy. Journal of the American Chemical Society, 2010, 132, 13692-13701.	6.6	649
9	Selective increase in CO ₂ electroreduction activity at grain-boundary surface terminations. Science, 2017, 358, 1187-1192.	6.0	596
10	Grain-Boundary-Dependent CO ₂ Electroreduction Activity. Journal of the American Chemical Society, 2015, 137, 4606-4609.	6.6	583
11	Probing the Active Surface Sites for CO Reduction on Oxide-Derived Copper Electrocatalysts. Journal of the American Chemical Society, 2015, 137, 9808-9811.	6.6	516
12	Pd-Catalyzed Electrohydrogenation of Carbon Dioxide to Formate: High Mass Activity at Low Overpotential and Identification of the Deactivation Pathway. Journal of the American Chemical Society, 2015, 137, 4701-4708.	6.6	424
13	A Direct Grain-Boundary-Activity Correlation for CO Electroreduction on Cu Nanoparticles. ACS Central Science, 2016, 2, 169-174.	5.3	362
14	The future of low-temperature carbon dioxide electrolysis depends on solving one basic problem. Nature Communications, 2020, 11, 5231.	5.8	336
15	Carbon dioxide utilization via carbonate-promoted Câ \in "H carboxylation. Nature, 2016, 531, 215-219.	13.7	318
16	Controlling H ⁺ vs CO ₂ Reduction Selectivity on Pb Electrodes. ACS Catalysis, 2015, 5, 465-469.	5.5	294
17	Reaction discovery enabled by DNA-templated synthesis and in vitro selection. Nature, 2004, 431, 545-549.	13.7	248
18	Carbon Monoxide Gas Diffusion Electrolysis that Produces Concentrated C2 Products with High Single-Pass Conversion. Joule, 2019, 3, 240-256.	11.7	218

MATTHEW W KANAN

#	Article	IF	CITATIONS
19	Multistep Small-Molecule Synthesis Programmed by DNA Templates. Journal of the American Chemical Society, 2002, 124, 10304-10306.	6.6	156
20	Microstructural origin of locally enhanced CO2 electroreduction activity on gold. Nature Materials, 2021, 20, 1000-1006.	13.3	119
21	Interfacial Electric Field Effects on a Carbene Reaction Catalyzed by Rh Porphyrins. Journal of the American Chemical Society, 2013, 135, 11257-11265.	6.6	114
22	An Electric Field–Induced Change in the Selectivity of a Metal Oxide–Catalyzed Epoxide Rearrangement. Journal of the American Chemical Society, 2012, 134, 186-189.	6.6	108
23	A scalable carboxylation route to furan-2,5-dicarboxylic acid. Green Chemistry, 2017, 19, 2966-2972.	4.6	107
24	Bragg coherent diffractive imaging of single-grain defect dynamics in polycrystalline films. Science, 2017, 356, 739-742.	6.0	88
25	Electrostatic Control of Regioselectivity in Au(I)-Catalyzed Hydroarylation. Journal of the American Chemical Society, 2017, 139, 4035-4041.	6.6	64
26	Alkaline O ₂ reduction on oxide-derived Au: high activity and 4e ^{â^'} selectivity without (100) facets. Physical Chemistry Chemical Physics, 2014, 16, 13601-13604.	1.3	41
27	Electrostatic control of regioselectivity via ion pairing in a Au(<scp>i</scp>)-catalyzed rearrangement. Chemical Science, 2014, 5, 4975-4979.	3.7	39
28	Carbonate-Promoted Hydrogenation of Carbon Dioxide to Multicarbon Carboxylates. ACS Central Science, 2018, 4, 606-613.	5.3	30
29	A closed cycle for esterifying aromatic hydrocarbons with CO2 and alcohol. Nature Chemistry, 2019, 11, 940-947.	6.6	30
30	Polyamide monomers <i>via</i> carbonate-promoted C–H carboxylation of furfurylamine. Chemical Science, 2020, 11, 248-252.	3.7	21
31	Molecular catalysis at polarized interfaces created by ferroelectric BaTiO ₃ . Chemical Science, 2017, 8, 2790-2794.	3.7	20
32	Imaging the Hydrogen Absorption Dynamics of Individual Grains in Polycrystalline Palladium Thin Films in 3D. ACS Nano, 2017, 11, 10945-10954.	7.3	20
33	Carbonate-promoted C–H carboxylation of electron-rich heteroarenes. Chemical Science, 2020, 11, 11936-11944.	3.7	15
34	A framework for automated structure elucidation from routine NMR spectra. Chemical Science, 2021, 12, 15329-15338.	3.7	15
35	Point-of-Care Analysis of Blood Ammonia with a Gas-Phase Sensor. ACS Sensors, 2020, 5, 2415-2421.	4.0	13
36	Comparing Scanning Electron Microscope and Transmission Electron Microscope Grain Mapping Techniques Applied to Well-Defined and Highly Irregular Nanoparticles. ACS Omega, 2020, 5, 2791-2799.	1.6	11

#	Article	IF	CITATIONS
37	Phase Behavior That Enables Solvent-Free Carbonate-Promoted Furoate Carboxylation. Journal of Physical Chemistry Letters, 2020, 11, 7544-7551.	2.1	9
38	A High-T _g Polyamide Derived from Lignocellulose and CO ₂ . Macromolecules, 2021, 54, 9978-9983.	2.2	7
39	Editorial overview: Seeds for a bioenergy future. Current Opinion in Chemical Biology, 2017, 41, A1-A2.	2.8	0
40	Hypophosphite addition to alkenes under solvent-free and non-acidic aqueous conditions. Chemical Communications, 2022, 58, 2180-2183.	2.2	0